Time-of-flight secondary ion mass spectrometry analyses of vancomycin

Lin Du, Xiaohui Yang, Wenqiang Li, Haoying Li, Shanbao Feng, Rong Zeng, Bin Yu, Liangxing Xiao, Yu Liu, Mei Tu, and Heng-Yong Nie

Time-of-flight secondary ion mass spectrometry analyses of vancomycin

Lin Du[a)]
Department of Materials Science and Technology, Jinan University, Guangzhou, Guangdong 510632, China; Engineering Research Center of Artificial Organs and Materials, Ministry of Education, Jinan University, Guangzhou, Guangdong 510632, China; and Surface Science Western, The University of Western Ontario, 999 Collip Circle, London, Ontario N6G 0J3, Canada

Xiaohui Yang, Wenqiang Li, Haoying Li, Shanbao Feng, and Rong Zeng
Department of Materials Science and Technology, Jinan University, Guangzhou, Guangdong 510632, China and Engineering Research Center of Artificial Organs and Materials, Ministry of Education, Jinan University, Guangzhou, Guangdong 510632, China

Bin Yu and Liangxing Xiao
Nanfang Hospital, Southern Medical University, Guangzhou, Guangdong 510515, China

Yu Liu
Jiangsu Key Laboratory of Advanced Manufacturing Equipment and Technology of Food, School of Mechanical Engineering, Jiangnan University, Wuxi, Jiangsu 214122, China

Mei Tu[b)]
Department of Materials Science and Technology, Jinan University, Guangzhou, Guangdong 510632, China and Engineering Research Center of Artificial Organs and Materials, Ministry of Education, Jinan University, Guangzhou, Guangdong 510632, China

Heng-Yong Nie[b)]
Surface Science Western, The University of Western Ontario, 999 Collip Circle, London, Ontario N6G 0J3, Canada and Department of Physics and Astronomy, The University of Western Ontario, London, Ontario N6A 3K7, Canada

As an antibiotic that prevents and treats infections caused by Gram-positive bacteria such as *Staphylococcus aureus*, vancomycin incorporated in a biodegradable polymer poly(lactide-*co*-glycolide) provides opportunities to construct controlled-release drug delivery systems. Developments associated with this promising system have been largely concentrated on areas of drug delivery kinetics and biodegradability. In order to provide surface analytical approaches to this important system, the authors demonstrate applicability of time-of-flight secondary ion mass spectrometry (TOF-SIMS) in three-dimensional molecular imaging for a model system consisting of alternating layers of ploy(lactide-*co*-glycolide) and vancomycin. TOF-SIMS imaging clarified that the two chemicals can undergo phase separation when dimethyl sulfoxide is used as the solvent. The authors identified two diagnostic ions that are abundant and structural moieties of vancomycin. The results on TOF-SIMS imaging and depth profiling vancomycin provide useful information for further applications of TOF-SIMS in the development of antibiotic drug delivery systems involving the use of vancomycin. *Published by the AVS.* https://doi.org/10.1116/1.5016186

I. INTRODUCTION

Gram-positive bacteria are characterized by a cell wall composed of a cross-linked peptidoglycan layer, which is constructed by alternating molecules of *N*-acetylglucosamine and *N*-acetylmuramic acid (NAM) connected via a glycoside bond.[1] These connected chains of the two monosaccharides are cross-linked by short chain peptides with one end bonded to NAMs and the other terminated by D-Ala-D-Ala. Vancomycin,[2] a glycopeptide, binds to five specific sites of the D-Ala-D-Ala moiety, preventing the short chain peptides from being cross-linked together by DD-transpeptidase, thus inhibiting or weakening the synthesis of the cell wall.[3–5] The result of these interactions eventually leads to cell death, which is why vancomycin is an antibiotic to Gram-positive bacteria, noticeably *Staphylococcus aureus*.[1] Injection or oral administration of antibiotics into the human body lacks temporary and distribution control, leading to over dosage and long-term accumulation of the drug agent in the body, which may cause various side effects. In order to counter these adversary effects, controlled-release drug delivery systems consisting vancomycin and biodegradable polymers are being developed.[6,7] Due to the biodegradability and ease of tailoring degradation kinetics by adjusting the ratio of the lactide and glycolide moieties, poly(lactide-*co*-glycolide) (PLGA) is a copolymer of choice for the biodegradable polymer matrix in controlled-release drug delivery systems.[8] We

[a)]Present address: Guangzhou Yueqing Regenerative Medical Science and Technology Ltd., 12-#307 Yuyan Street, Luogang District, Guangzhou, Guangdong 510663, China.
[b)]Authors to whom correspondence should be addressed; electronic addresses: tumei@jnu.edu.cn; hnie@uwo.ca

have reported vancomycin-loaded PLGA microspheres and scaffolds for controlled-release drug delivery systems.[9,10] The scaffold approach is especially promising in bone regeneration as scaffold provides mechanical support for cell growth and the loaded biomolecules and antibiotics enhance tissue formation and prevent infections.[11,12] For such drug-loaded polymer matrix systems, *in vitro* and *in vivo* drug release kinetics and biodegradability, as well as their applications, have been extensively explored.[13,14] The success of this controlled-release drug delivery system is important in vancomycin applications to fight diseases caused by Gram-positive bacteria.

The surface chemistry of a scaffold composed of vancomycin-loaded PLGA microspheres is important to control the performance of the system in delivering drugs in a controlled manner both temporarily and in distribution. However, investigations concentrated on surface analysis of these two materials are scarce. For the purpose of developing analytical approaches to study vancomycin, we make use of time-of-flight secondary ion mass spectrometry (TOF-SIMS),[15] which is especially powerful in revealing chemical information.[16–20] TOF-SIMS has been applied in depth profiling multilayer drug-loaded beads,[21] drug-eluting coatings on implantable stents[22,23] and other drug-delivery systems,[24,25] as well as surface imaging of porous microspheres[26] of controlled-release drug delivery systems. In this technique, a pulsed (primary) ion beam (e.g., Bi_3^+) is used to bombard the surface of a specimen to generate (secondary) ions from the topmost monolayer (1–3 nm). The imaging capability of TOF-SIMS is especially powerful in answering not only the question of what is on the surface but also the question of how molecules are distributed over the surface. With another ion beam (e.g., C_{60}^+) serving to sputter a controllable amount of substance from the surface, chemical variations in the depth direction can also be accessed.[16] Therefore, TOF-SIMS provides three-dimension molecular information, which is powerful in exploring drug-loaded polymeric systems.

Liquid chromatography-mass spectrometry (LC-MS) has been used to investigate vancomycin, with doubly charged and doubly protonated ions being the diagnostic ion for vancomycin.[27–29] However, this method lacks imaging and depth profiling capabilities. Despite the fact that vancomycin is an antibiotic that has been extensively studied, to our knowledge, there have been no TOF-SIMS studies on vancomycin and identification of diagnostic ions. In order to demonstrate the applicability of TOF-SIMS in providing three-dimensional molecular information, we select a model system of layered structure of PLGA and vancomycin. We examine the fragmentation of vancomycin in TOF-SIMS and identify diagnostic ions that are abundant and structural moieties. In this article, we show that the depth profiling of the layered structure of the two molecules, as well as their phase separation revealed by imaging. The demonstrated TOF-SIMS applications are expected to promote TOF-SIMS applications in areas related to controlled-release drug delivery systems.

II. MATERIALS AND METHODS

The vancomycin hydrochloride used in this study was a product for injection produced by Zhejiang Medicine Co., Ltd., China. The molar mass of vancomycin ($C_{66}H_{75}Cl_2N_9O_{24}$) is 1449.3 Da with its monoisotopic molar mass being 1447.4302 Da. (The molecular structure of vancomycin is shown in Fig. 4.) Poly ($_{D,L}$-lactide-*co*-glycolide) (PLGA) (65:35) (BLYCL2015062501) from Shenzhen Polymtek Biomaterial Co., Ltd., Shenzhen, China, was used in this experiment. Deionized water and dichloromethane (DCM) were used to make aqueous vancomycin solution and PLGA solution in DCM, respectively. The concentration for both solutions were 2 wt. %. A multilayer PLGA/vancomycin/PLGA/Si sample was prepared by spin-coating (4000 rpm) the solutions alternatively on a Si substrate. We also used dimethyl sulfoxide (DMSO) to dissolve both PLGA and vancomycin and placed the solution on a mica substrate, which resulted in phase separation between the two chemicals.

The surface morphology of the vancomycin and PLGA layers was examined using the dynamic force mode AFM (Park Systems XE-100, Korea). In this mode, a cantilever with a nominal spring constant of 40 N/m and a resonant frequency of 300 kHz (NSC15, MikroMasch, Sofia, Bulgaria) is vibrated at a frequency slightly below the resonant frequency. When the tip engages the sample surface, its amplitude reduces due to the tip-sample interaction. Reduced amplitude (usually 50%–80% of that in free space) is used as the feedback parameter so that the system scans the sample according to its contour, rendering surface morphology. AFM images constructed with 256 scan lines with each line having 256 points were obtained in air at room temperature with a relative humidity of ~40%.

An IONTOF GmbH (Münster, Germany) TOF-SIMS IV equipped with a cluster bismuth liquid metal ion gun was employed to examine the surface of PLGA and vancomycin and depth profile a layered structure of PLGA/vancomycin/PLGA/Si. The high current bunched mode of the instrument was used in this study, which offers high mass resolutions with a lateral spatial resolution of a couple of microns. Although not used in this study, another mode of the instrument is the burst alignment mode, offering lateral spatial resolutions at submicrons with limited mass resolution and sensitivity. This mode would be used only when lateral spatial resolutions were the most important aspect in one's experiment.

The base pressure of the TOF-SIMS analytical chamber was about 1×10^{-8} mbar. The primary 25 keV Bi_3^+ cluster ion beam pulsed at ~1 ns (target current of ~1 pA) bombarded the sample surface, generating secondary ions. Either positive or negative ions were extracted (depending on the selection of the polarity of electric field), mass separated and detected via a reflectron type of time of flight analyzer, followed by a pulsed, low energy (~18 eV) electron flood used to neutralize sample charging. This cycle of starting a shot of the primary ion to completion of the charge compensation was either 100 or 140 μs to collect ions with mass to charge ratio (m/z) up to 900 or 1600, respectively.
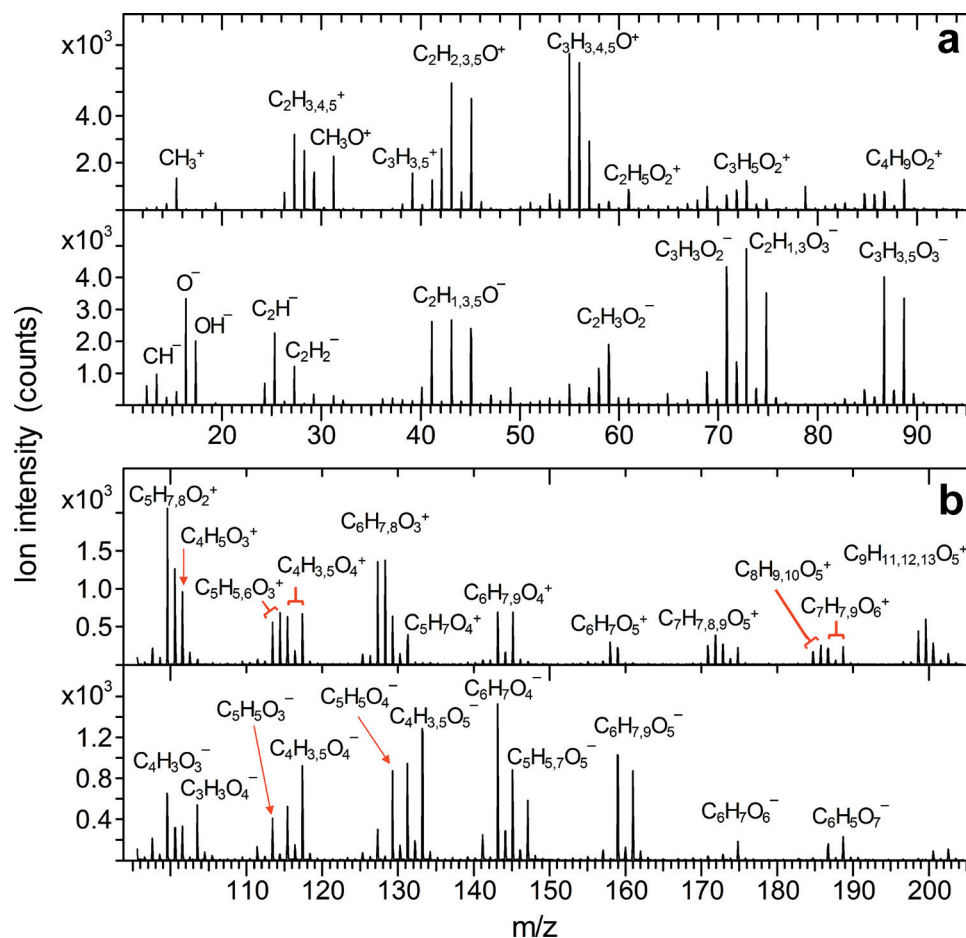
FIG. 1. Positive and negative secondary ion mass spectra of PLGA in m/z (a) 11–95 and (b) 95–205. Due to crowded ions shown in (b), red markers are used to connect the identified ions and their corresponding peaks.

Negative and positive secondary ion mass spectra were collected on the surface over an area of $200 \times 200\ \mu\text{m}^2$ with a pixel density of 128×128. The primary ion dosage was approximately 6×10^{11} ions/cm^2, which was well below the static limit of $\sim 10^{13}$ ions/cm^2.[16,30] Secondary ion mass spectra were initially calibrated using hydrogen, carbon and hydrocarbon ions. In order to establish a more accurate mass scale for PLGA and vancomycin, the spectra were recalibrated using known higher-mass species from the two chemicals. Mass resolutions for C_4H^- (m/z 49), $C_3H_3O_3^-$ (87), $C_2H_3^+$ (27), and $C_3H_4O^+$ (56) were 4300, 6900, 4100, and 8800, respectively. The fidelity of the assignment is quantified by the deviation, in parts per million (ppm), of the peak from the assigned chemical formula $\Delta = 10^6 \times (M_{\text{peak}} - M_{\text{assigned}})/M_{\text{assigned}}$.

Depth profiles were obtained on a multilayer sample by alternatively sputtering the surface in an area of $400 \times 400\ \mu\text{m}^2$ using a 10 keV C_{60}^+ ion beam (target current $\sim$0.2 nA) for 1 s followed by analyzing the surface using the Bi_3^+ primary ion beam over an area of $200 \times 200\ \mu\text{m}^2$ within the sputtered area. The depths of the craters generated were measured using a profilometer (P-10, KLA-Tencor) to calibrate the sputter depth. At each sputtered depth, a full spectrum was collected at each of the 128×128 pixels over the rastered area, from which ion images were obtained by plotting the intensities of selected ions against the rastered pixels.

III. RESULTS AND DISCUSSION

A. Identification of diagnostic ions of vancomycin

Since the identification of chemical structure of an ion requires a precise calibration of the peak in an ion mass spectrum, a good way to do it is to use two known ions each having a lower and higher m/z than the ion to be identified. The strategy to identify diagnostic ions from vancomycin is to make use of PLGA ions, which are readily identifiable from its lactide ($C_3H_4O_2$) and glycolide ($C_2H_2O_2$) moieties.[26] PLGA ions are useful in precisely calibrating the spectra so that our identification of vancomycin can be done with more credence when using a mixture of the two chemicals. We first show in Figs. 1(a) and 1(b) the positive and negative secondary ion mass spectra of pure PLGA in m/z 11–95 and 95–205, respectively. There are numerous characteristic ions from PLGA, or more precisely, from its lactide and glycolide moieties. The ions characteristic of PLGA are $[nM+O\pm H]^-$ and $[nM-OH]^+$. Examples of abundant ions are $C_2H_2O^+$ (m/z 43), $C_2H_5O^+$ (45), $C_3H_3O^+$ (55), $C_5H_7O_2^+$ (99), $C_6H_7O_3^+$ (127), $C_6H_8O_3^+$ (128), $C_6H_7O_4^+$ (143), and
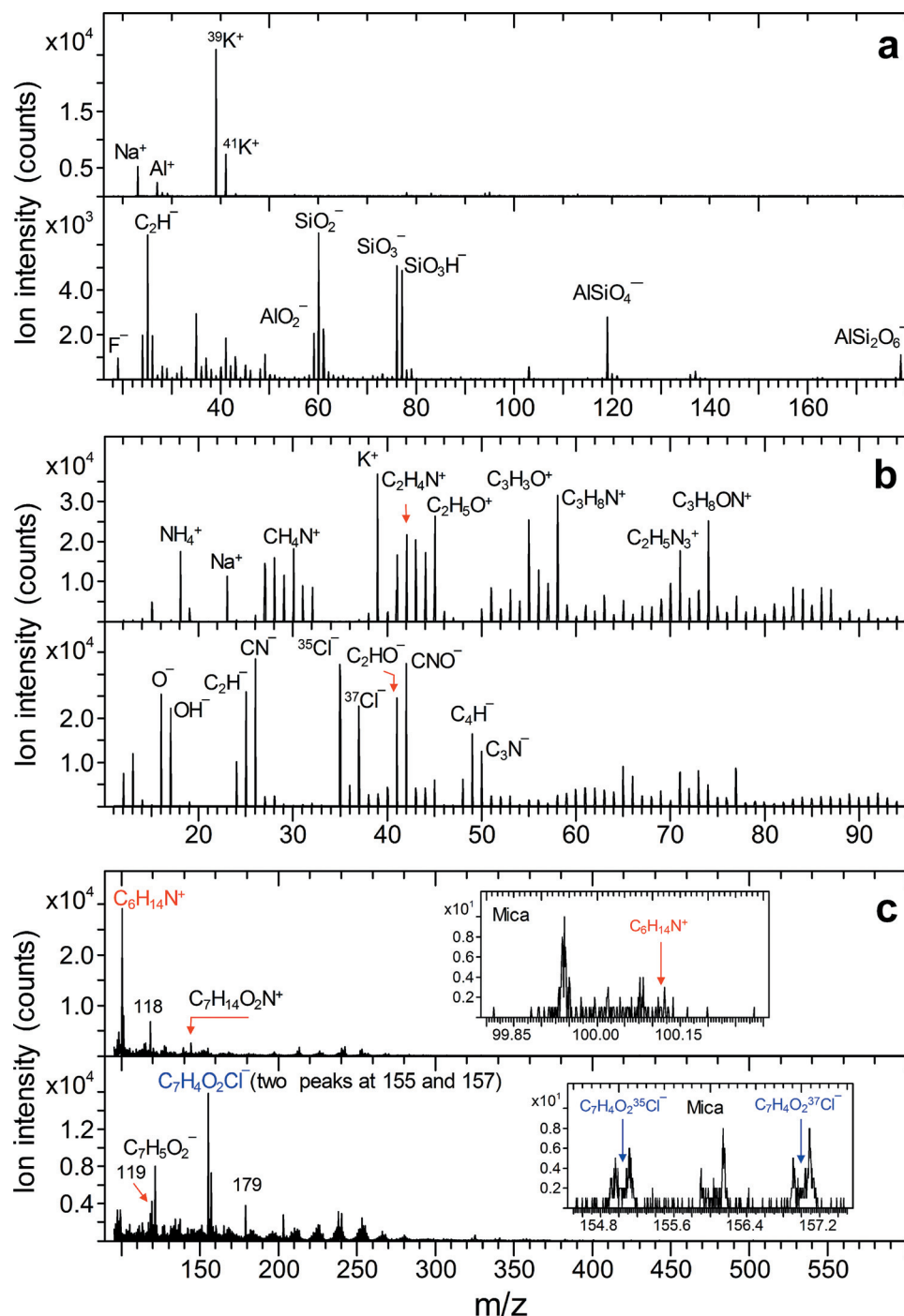
FIG. 2. Positive and negative secondary ion mass spectra of a cleaved Muscovite mica substrate in *m/z* 18–180 (a) and vancomycin film deposited on a mica substrate in *m/z* 11–95 (b) and 95–600 (c). Arrows in (b) and (c) connect the ions to their corresponding peaks. Inserted in (c) are mass spectra of the mica substrate at *m/z* range 99.8–100.3 (upper panel) and 154.7–157.3 (lower panel), showing the lack of peaks at the positions of $C_6H_{14}N^+$ and $C_7H_4O_2{}^{35}Cl^-$ and $C_7H_4O_2{}^{37}Cl^-$, respectively.

$C_9H_{12}O_5{}^+$ (199). Abundant negative ions include $C_3H_3O_2{}^-$ (71), $C_2HO_3{}^-$ (73), $C_2H_3O_3{}^-$ (75), $C_3H_3O_3{}^-$ (87), $C_3H_5O_3{}^-$ (89), $C_4H_5O_4{}^-$ (117), $C_4H_5O_5{}^-$ (133), $C_6H_7O_4{}^-$ (143), and $C_6H_7O_5{}^-$ (159).

An aqueous solution of vancomycin was spin-coated on cleaved Muscovite mica, which offers an atomically flat, hydrophilic surface. In order to understand how the mica substrate affects the TOF-SIMS results of a vancomycin film prepared on it, we show in Fig. 2(a) the positive (upper

panel) and negative (lower panel) secondary ion mass spectra of a cleaved mica substrate in *m/z* 11–200. It is clear that potassium ions dominate the positive ion mass spectrum. While in the negative ion mass spectrum, the abundant ions are C_2H^- (25), $SiO_2{}^-$ (60), $SiO_3{}^-$ (76), SiO_3H^- (77), $AlSiO_4{}^-$ (119), and $AlSi_2O_6$ (179).

Shown in Fig. 2(b) are positive and negative secondary ion mass spectra of vancomycin in *m/z* 11–95. Since the vancomycin film was spin-coated on the surface of cleaved

Muscovite mica, we first check whether there are mica constituent entities appearing in the spectra. The abundant K^+ detected is from the mica substrate, which is potassium aluminum silicate hydroxide fluoride and may be expressed as $KAl_2(AlSi_3O_{10})(F, OH)_2$. The potassium ions are present between the silicate sheets.[31] We noticed that negative ions from the mica substrate, such as SiO_2^-, SiO_3^-, and SiO_3H^- are relatively weak in the negative secondary ion mass spectrum of the vancomycin film [lower panel in Fig. 2(b)]. We can also confirm that the negative ion peaks at m/z 119 and 179 in the lower panel of Fig. 2(c), assigned to $AlSiO_4^-$ and $AlSi_2O_6^-$, respectively, are from the mica substrate. Therefore, the impact of the mica substrate on the TOF-SIMS results of the vancomycin film deposited on it was minimal.

Because TOF-SIMS probes only the top 1–3 nm, the detection of those mica constituent entities indicates either the vancomycin layer is as thin as a couple of nanometers or the layer is porous. In our case, we confirmed using AFM that the vancomycin is free from porosity, thus verifying that the thickness of the vancomycin layer is indeed only a couple of nanometers.

The most abundant positive and negative ions from vancomycin in m/z 11–95, as shown in Fig. 2(b), are CH_2N^+ (28), CH_4N^+ (30), $C_2H_4N^+$ (42), $C_3H_6N^+$ (56), $C_3H_8N^+$ (58), $C_2H_5N_3^+$ (71), $C_3H_8ON^+$ (74), CN^- (26), $^{35}Cl^-$ (35), $^{37}Cl^-$ (37), CNO^- (42), and C_3N^- (50), respectively. Vancomycin contains nitrogen and chlorine so that CN^-, CNO^-, and Cl^- ought to be diagnostic ions. However, if vancomycin is presented in an environment composed of other materials containing nitrogen and chlorine, then CN^-, CNO^-, and Cl^- will no longer be diagnostic. Therefore, ions associated with more structural information of vancomycin are needed for identification of the chemical. As shown in Fig. 2(c), there is an abundant positive ion at m/z 100, which is assigned to $C_6H_{14}N^+$. On the other hand, we confirmed that the two abundant negative ions at m/z 155 and 157

resemble the isotope pattern of chlorine, allowing us to assign them to $C_7H_4O_2^{35}Cl^-$ and $C_7H_4O_2^{37}Cl^-$, respectively. The details on these identifications are shown in Fig. 3 and discussed below. We confirmed that, from the inserted spectra of the cleaved mica substrate in Fig. 2(c), these peaks are not related to the mica substrate.

In order to more precisely calibrate the m/z values of those three ions, we make use of the known ion species of PLGA by using a sample with a mixture of vancomycin and PLGA. Shown in Fig. 3(a) are positive ion mass spectra obtained from a PLGA layer (upper panel) and a mixture of vancomycin and PLGA (lower panel), both prepared on a Si wafer. Both positive ion spectra were calibrated using known PLGA ions of $C_3H_3O^+$ (55) and $C_6H_7O_3^+$ (127). The vancomycin ion at m/z 100.1131, in the lower panel of Fig. 3(a), is assigned to $C_6H_{14}N^+$, with a deviation of 5 ppm. The two PLGA ions at m/z 100 are assigned to $C_4H_4O_3^+$ and $C_5H_8O_2^+$. The vancomycin ion $C_6H_{14}N^+$ is well resolved from the two PLGA ions $C_4H_4O_3^+$ and $C_5H_8O_2^+$. As shown in Fig. 4, $C_6H_{14}N^+$ is a structural moiety of vancomycin, whose chemical structure is depicted in Fig. 4, where the structure of vancomycin and other identified ions are depicted.

Through precisely calibrating the negative spectra using the two PLGA ions $C_6H_7O_4^-$ (143) and $C_6H_7O_5^-$ (159), the two vancomycin ions at m/z 154.9908 and 156.9880 were assigned to $C_7H_4O_2^{35}Cl^-$ and $C_7H_4O_2^{37}Cl^-$, respectively, with deviations of 5 ppm. Both the m/z and ion intensity ratio of these two ions match precisely the isotopic distribution of $C_7H_4O_2Cl$, whose chemical structures are depicted in Fig. 4. The ion $C_7H_4O_2Cl^-$ is readily explained by the two identical phenyl groups containing a chorine atom. At the same nominal m/z 155 and 157, there are two PLGA ions, which are assigned to $C_7H_7O_4^-$ and $C_7H_9O_4^-$, respectively. Those two PLGA ions have m/z 0.0438 and 0.0626 larger than the two vancomycin ions, respectively.
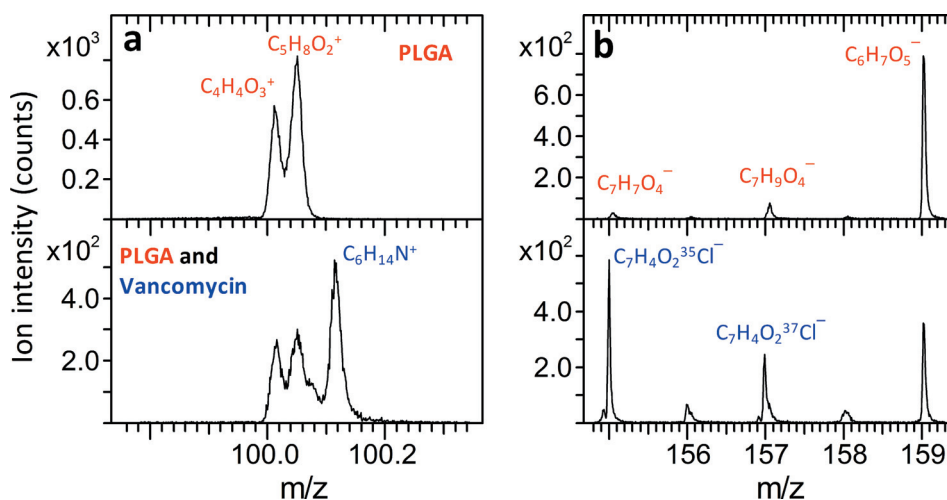

FIG. 3. Positive (a) and negative (b) secondary ion mass spectra for pure PLGA and (upper panels) and their mixture (lower panels), showing the vancomycin diagnostic ions at $C_6H_{14}N^+$, $C_7H_4O_2^{35}Cl^-$, and $C_7H_4O_2^{37}Cl^-$ at m/z 100, 155, and 157, respectively. Also shown are PLGA ions $C_4H_4O_3^+$ and $C_5H_8O_2^+$ at m/z 100, $C_7H_7O_4^-$ at m/z 155, and $C_7H_9O_4^-$ at m/z 157. The PLGA ion $C_6H_7O_5^-$ at m/z 159 is useful in calibrating the negative ion mass spectrum for the mixture of vancomycin and PLGA to acquire accurate m/z for the two vancomycin ions at m/z 155 and 157.
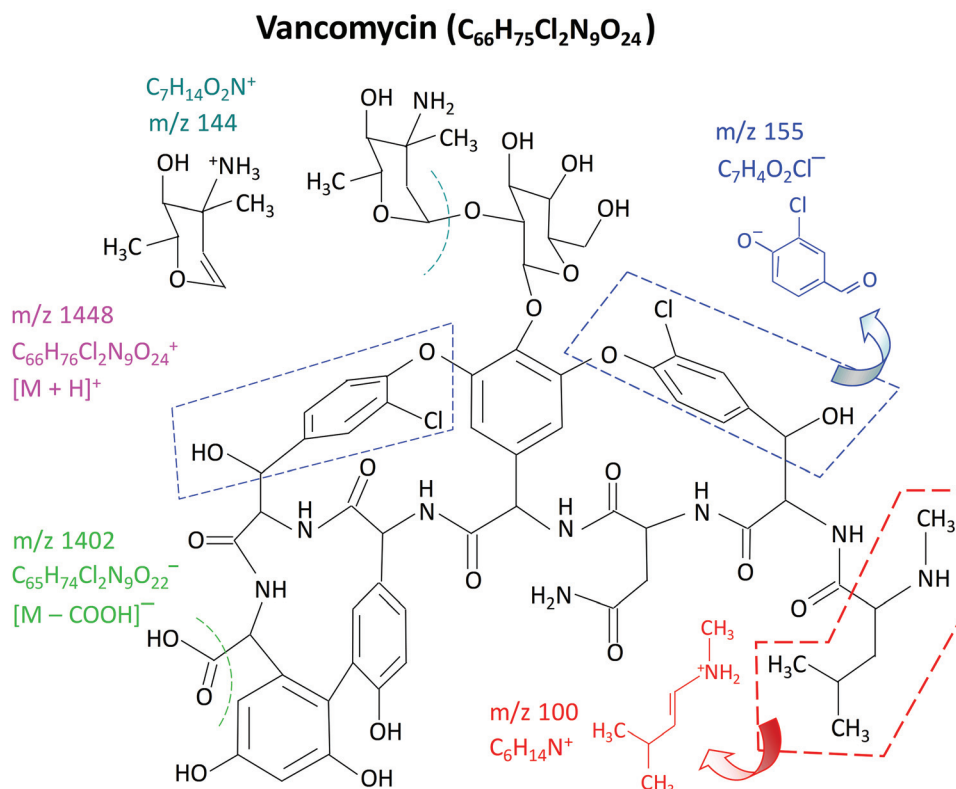
Vancomycin ($C_{66}H_{75}Cl_2N_9O_{24}$)

FIG. 4. Chemical structures of vancomycin and the two vancomycin ions $C_6H_{14}N^+$ and $C_7H_4O_2Cl^-$. The protonated and decarboxylated molecular ions, i.e., $C_{66}H_{76}Cl_2N_9O_{24}^+$ and $C_{65}H_{74}Cl_2N_9O_{22}^-$, are also depicted, where M represent the molecular formula $C_{66}H_{75}Cl_2N_9O_{24}$. Also depicted is an ion $C_7H_{14}O_2N^+$ fragmented from the vancosamine end.

The weak peak of a positive ion at *m/z* 144 in Fig. 2(c) is also known to be $C_7H_{14}O_2N^+$ from LC-MS.[27,29] which is the vancosamine moiety as depicted in Fig. 4. It is worth pointing out that in contrast to TOF-SIMS, $C_7H_{14}O_2N^+$ is a rather abundant peak in LC-MS.[27,29] We also tried identifying other peaks that are not as abundant as $C_6H_{14}N^+$ and $C_7H_4O_2Cl^-$. For example, the negative ion at *m/z* 121 is assigned to $C_7H_5O_2^-$. This negative ion may be due to the benzene ring with two hydroxyls when its bond with the adjacent benzene ring breaks and the carbon atom beside the carboxyl group cleaves. On the other hand, the positive ion peak at *m/z* 118 can be assigned to $C_5H_{12}O_2N^+$ on the basis of mass matching. However, we have not yet found a corresponding structural moiety in vancomycin. Because we have the abundant and structurally relevant ions of $C_6H_{14}N^+$ and $C_7H_4O_2Cl^-$, perhaps $C_5H_{12}O_2N^+$ and $C_7H_5O_2^-$, which are much less abundant, will not be needed for identifying vancomycin, especially when the protonated molecular ion can be detected. The protonated and decarboxylate molecular ions $C_{66}H_{76}Cl_2N_9O_{24}^+$ and $C_{65}H_{74}Cl_2N_9O_{22}^-$, which will be discussed later, are also depicted in Fig. 4.

Figure 5(a) shows both positive and negative ion mass spectra of vancomycin in *m/z* 600–1480, which are calibrated using ions including the identified ions of CH_3^+, $C_3H_5^+$, and $C_6H_{14}N^+$, and C^-, C_4H^-, and $C_7H_4O_2Cl^-$, respectively. The two peaks at *m/z* 1448.4176 and 1402.4215 in Fig. 5(a) are identified as $C_{66}H_{76}Cl_2N_9O_{24}^+$ and $C_{65}H_{74}Cl_2N_9O_{22}^-$ with deviations of −14 and −8 ppm,

respectively. With M representing vancomycin molecular formula, $C_{66}H_{76}Cl_2N_9O_{24}^+$ can be denoted as $[M+H]^+$. This positive ion corresponds to protonated vancomycin molecular ion. As shown in Fig. 4, $C_{65}H_{74}Cl_2N_9O_{22}^-$ corresponds to $[M-COOH]^-$, that is, with the removal of the carboxyl group COOH from the vancomycin molecule. This negative ion may be termed as "decarboxylated" vancomycin molecular ion.

The *m/z* range used in Fig. 5(a) does not allow to show the isotope patterns of the $[M+H]^+$ and $[M-COOH]^-$ ions. Shown in the upper panel of Figs. 5(b) and 5(c) are the measured isotope patterns of $[M+H]^+$ and $[M-COOH]^-$, with their monoisotopic[32] peaks at *m/z* 1448 and 1402, respectively. The simulated isotope patterns of the corresponding ions are shown in the lower panels of Figs. 5(b) and 5(c), respectively. It is clear that the theoretical and experimental isotopic distributions match. The isotopic pattern shown in Fig. 5(b) has also been observed by Orbitrap.[32,33]

Vancomycin has been investigated using LC-MS, in which the base peak is $C_7H_{14}O_2N^+$, the vancosamine end group in the glycoside group of vancomycin, with $C_{13}H_{25}O_7N^+$ (307) corresponding to the glycoside group having a much smaller abundance.[27] In the LC-MS investigation, an abundant peak at *m/z* 725 is identified as $[M+2H]^{2+}$.[27–29] By comparison, vancomycin is fragmented quite differently in TOF-SIMS. For example, nothing is detected at *m/z* 725. In TOF-SIMS $C_7H_{14}O_2N^+$ is detected, but not $C_{13}H_{25}O_7N^+$. While $C_7H_{14}O_2N^+$ is abundant in LC-
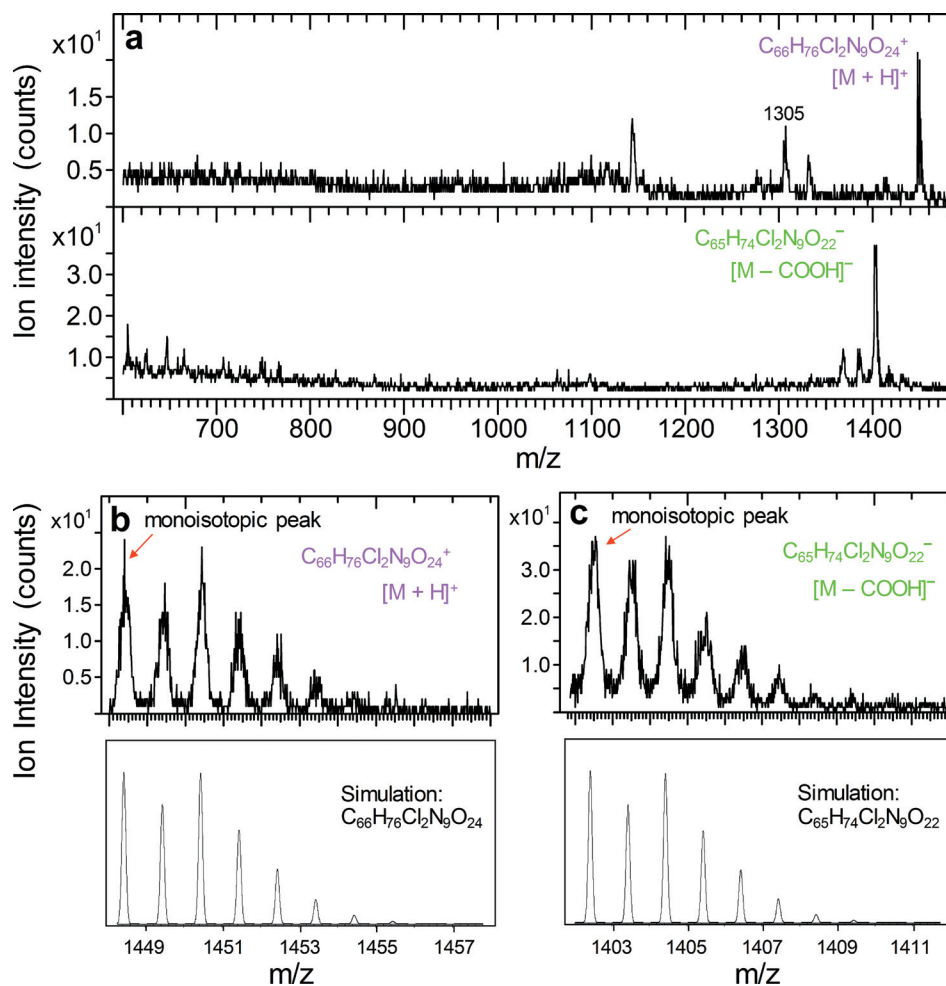
FIG. 5. Positive and negative secondary ion mass spectra of vancomycin (a) in m/z 600–1500. The upper panels of (b) and (c) are positive and negative secondary ion spectra showing the isotopic distributions of $C_{66}H_{76}Cl_2N_9O_{24}^+$ and $C_{65}H_{74}Cl_2N_9O_{22}^-$, with their monoisotopic peak at m/z 1448 and 1402, respectively. M in (b) and (c) represents the vancomycin molecular formula $C_{66}H_{75}Cl_2N_9O_{24}$. The simulated isotopic distribution of $C_{66}H_{76}Cl_2N_9O_{24}$ and $C_{65}H_{74}Cl_2N_9O_{22}$ are shown in the lower panels of (b) and (c), respectively.

MS,[27,29] in TOF-SIMS, it is much weaker than $C_6H_{14}N^+$. To our knowledge, $C_6H_{14}N^+$ has never been mentioned in the literature when LC-MS was used to study vancomycin, indicating that this ion is either not generated or very weak in LC-MS.

In a LC-MS study on understanding ion fragmentation of vancomycin, precursor deprotonated vancomycin ion $[M-H]^-$ in further MS collision-induced dissociation (CID)

experiment resulted in decarboxylate vancomycin ion $C_{65}H_{74}Cl_2N_9O_{22}^-$.[27] On the other hand, the CID spectrum of precursor protonated vancomycin ion $[M+H]^+$ resulted in an abundant peak at m/z 1305, which corresponds to the loss of its vancosamine end group that makes the positive ion peak at m/z 144.[27] As shown in Fig. 5(a), we also detected this ion at m/z 1305, or more precisely, a group of ions reflecting the isotopic distribution (details not shown). It can

TABLE I. Ions identified for vancomycin with positive ions recalibrated using CH_3^+, $C_3H_5^+$ and $C_6H_{14}N^+$ and negative ions using C^-, C_4H^- and $C_7H_4O_2Cl^-$.

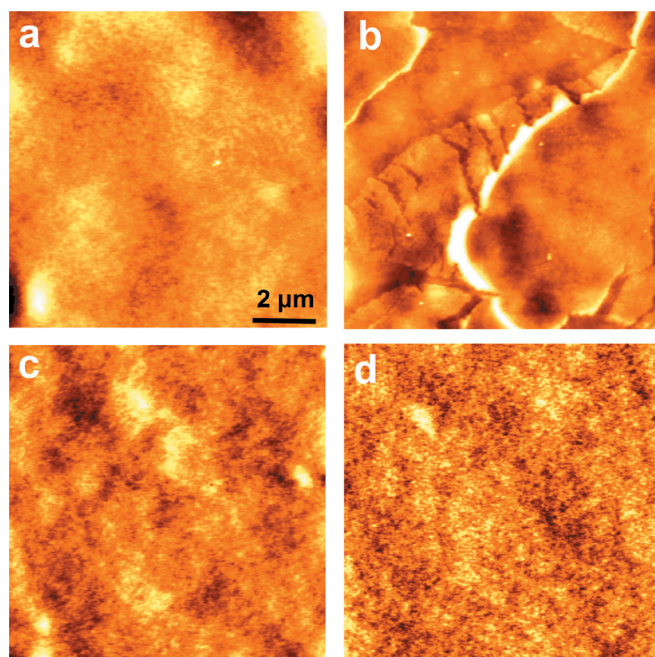| Positive ion	m/z	Δ (ppm)	Intensity (%)	Negative ion	m/z	Δ (ppm)	Intensity (%)
CH_2N^+	28.0198	38	38	CN^-	26.0053	85	100
CH_4N^+	30.0354	33	44	Cl^-	34.9712	66	95
$C_2H_4N^+$	42.0357	31	61	CNO^-	41.9999	45	99
$C_2H_6N^+$	44.0531	70	46	C_3N^-	50.0040	18	19
$C_3H_8N^+$	58.0683	45	100	$C_7H_5O_2^-$	121.0261	−24	13
$C_3H_8ON^+$	74.0638	43	85	$C_7H_4O_2Cl^-$	154.9903	2	34
$C_6H_{14}N^+$	100.1132	6	74	$C_{65}H_{74}Cl_2N_9O_{22}^-$	1402.4215	−8	<0.1
$C_7H_{14}O_2N^+$	144.1055	21	4				
$C_{66}H_{76}Cl_2N_9O_{24}^+$	1448.4176	−14	<0.1				

FIG. 6. AFM images for (a) the PLGA layer coated on a Si substrate, (b) the vancomycin layer coated on the PLGA layer, and (c) the topmost PLGA layer coated on the vancomycin layer. Shown in (d) is an AFM image for a vancomycin layer spin-coated on a cleaved mica. The height range for (a)–(d) is 5.4, 11.5, 2.3, and 1.9 nm, respectively.

be seen that TOF-SIMS captures these high mass ions, except for the deprotonated vancomycin ion, as the LC-MS does.

Summarized in Table I are the major vancomycin ions, their measured m/z and deviations obtained from ion mass spectra recalibrated using three ions of CH_3^+, $C_3H_5^+$, and $C_6H_{14}N^+$ for positive ions and C^-, C_4H^-, and $C_7H_4O_2Cl^-$ for negative ions, respectively. The intensities of the ions listed in the table are normalized to that of the most abundant ions of $C_3H_8N^+$ and CN^- for positive and negative ions, respectively. It can be seen that the intensity of $C_6H_{14}N^+$ is three quarters of that of $C_3H_8N^+$, while the intensity of $C_7H_4O_2Cl^-$ is one third of that of CN^-, showing that these diagnostic ions are also abundant. On the other hand, the protonated and decarboxylated vancomycin molecular ions, $C_{66}H_{76}Cl_2N_9O_{24}^+$ and $C_{65}H_{74}Cl_2N_9O_{22}^-$, are weak, with their intensities being less than one thousandth of those of $C_3H_8N^+$ and CN^-, respectively.

B. Depth profiling PLGA/Vancomycin/PLGA

A multilayered sample of PLGA/vancomycin/PLGA made by subsequently spin-coating their respective solutions on a Si substrate. Shown in Figs. 6(a)–6(c) are AFM images ($10 \times 10 \mu m$) of the first PLGA layer, the vancomycin layer coated on the first PLGA layer and the topmost PLGA layer, respectively. The root mean square roughness for the three layers starting with the first layer is 0.4, 1.0 and 0.2 nm for the AFM images in Figs. 6(a)–6(c), respectively. The two PLGA layers are similar and featureless. By contrast, there are stripelike features seen on the surface of the vancomycin

layer coated on the first PLGA layer. We consider that the structures observed are due to the fact that PLGA is hydrophobic while vancomycin hydrophilic (its aqueous solution was used for the spin-coating). We tested this hypothesis by spin-coating aqueous solution of vancomycin on cleaved mica, which is a hydrophilic surface as it is terminated by oxygen groups (and potassium ions).[31] As shown in Fig. 6(d) the vancomycin layer is smooth, with a root mean square roughness of only 0.2 nm. Because elements of the underneath mica were detected from the surface of the vancomycin layer, we believe that it is perhaps close to a monolayer.

The multilayer PLGA/vancomycin/PLGA spin-coated on a Si substrate [Fig. 7(a)] was depth profiled using a 10 keV C_{60}^+ sputter ion beam. We verified that there are numerous ion species that are suitable for depth profiling the layered structure. The intensity of the monoisotopic[27] decarboxylated ion $C_{65}H_{74}Cl_2N_9O_{22}^-$ is 1/300 of that of $C_7H_4O_2Cl^-$. Therefore, due to the lack of abundance, the decarboxylated molecular ion is perhaps not suitable for depth profiling. For clarity purposes, we present in Fig. 8(b) depth profiles of Cl^-, CN^-, $C_7H_4O_2{}^{35}Cl^-$, and $C_7H_4O_2{}^{37}Cl^-$ for vancomycin and $C_2H_3O_3^-$ and $C_3H_3O_3^-$ for the glycolide and lactide moieties, respectively, of PLGA.

As shown in the depth profiles of $C_2H_3O_3^-$ and $C_3H_3O_3^-$ in Fig. 7(b), at the very center of the vancomycin layer, there are still signals corresponding to these two ions. By comparing the ion mass spectra of PLGA and vancomycin, we noticed that all PLGA peaks have either the same ion or a different ion having the same nominal m/z from vancomycin. In fact, vancomycin has ions $C_6H_3^-$ and C_6HN^- at the same m/z 75 and 87, making them interfere with PLGA ions $C_2H_3O_3^-$ and $C_3H_3O_3^-$, respectively. The m/z differences between the two peaks at m/z 75 and 87 are only 0.0153 and 0.0027, respectively. The apparent signals of peaks at m/z 75 and 87 within the vancomycin layer are thus contributed from $C_6H_3^-$ and C_6HN^-, rather than $C_2H_3O_3^-$ and $C_3H_3O_3^-$. It is thus important to check the ion mass spectrum when processing the depth profile data for layered structures. This can be readily done in TOF-SIMS since one can monitor both the depth profile and the mass spectrum. On the other hand, there are unique peaks for vancomycin, such as Cl^- and $C_7H_4O_2Cl^-$ that are not interfered by PLGA ions. We can confirm that depth profiles of positive ions of NH_4^+, $C_6H_{14}N^+$ for vancomycin and $C_3H_3O^+$ and $C_4H_5O_4^+$ for PLGA (not shown), resemble those of the depth profiles of negative ions presented in Fig. 7(b).

Shown in Fig. 7(c) are overlapped images of Cl^- (red, representing vancomycin) and $C_3H_3O_3^-$ (green, representing PLGA) depicting the cross section of the layered structure. Note that in Fig. 7(c) the horizontal dimension (200 μm) and vertical dimension (330 nm) are not to scale: the horizontal dimension represents the size of the rastered area and the vertical dimension the depth profiled.

We can also access ion images along the profiled depth. For example, presented in Figs. 7(d)–7(g) are images of Cl^- and $C_3H_3O_3^-$ for depths of 34, 103, 160, and 190 nm, respectively, as indicated by the arrowed lines between them
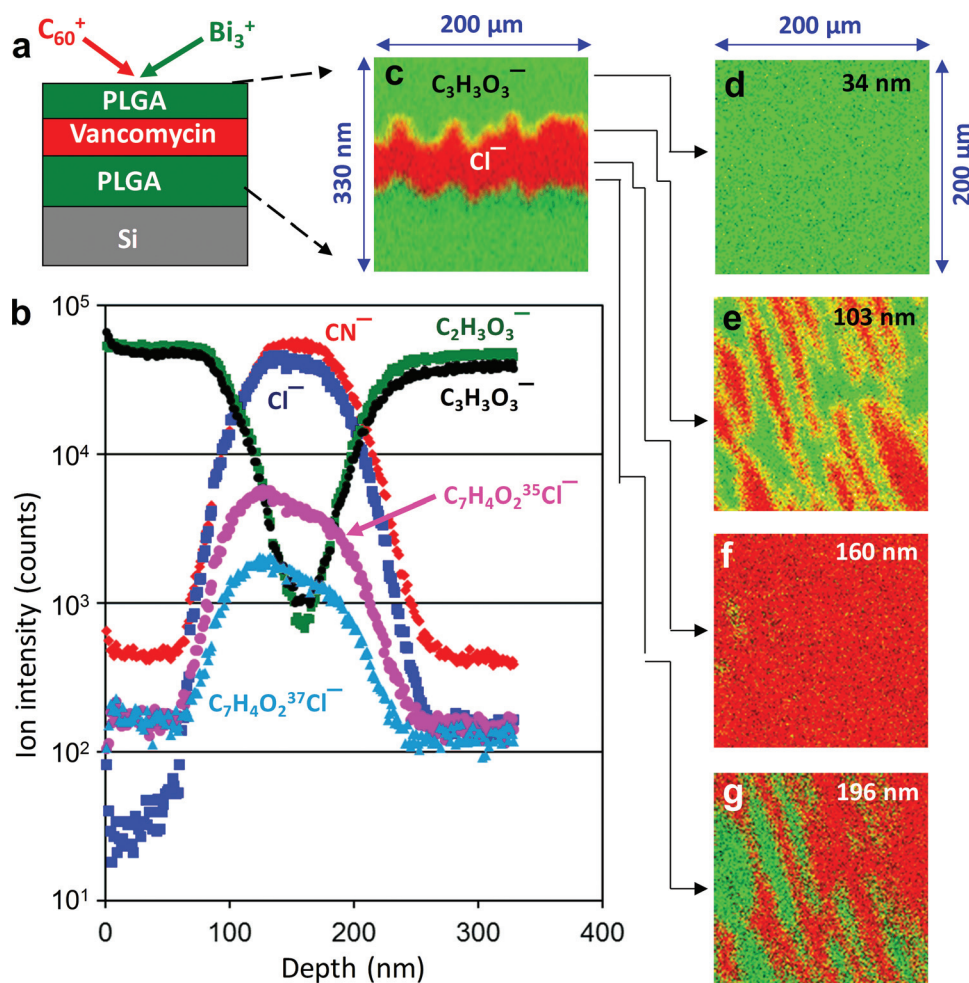
FIG. 7. Illustration of the PLGA/vancomycin/PLGA layers prepared on a Si wafer (a) and depth profiles (b) of ions CN^-, Cl^-, $C_7H_4O_2{}^{35}Cl^-$, and $C_7H_4O_2{}^{37}Cl^-$ representing vancomycin layer, as well as those of $C_2H_3O_3{}^-$ and $C_3H_3O_3{}^-$ representing the PLGA layers. Shown in (c) is a cross section of the layers expressed by intensities of $C_3H_3O_3{}^-$ (green in color) and Cl^- (red) for PLGA and vancomycin, respectively, with a probed depth of 330 nm over a rastered area of $200 \times 200\ \mu m^2$. The overlapped images of $C_3H_3O_3{}^-$ and Cl^- (d)–(g) show distributions of PLGA and vancomycin at probed depths of 34, 103, 160, and 196 nm, respectively.

and Fig. 7(c). The uneven vancomycin at the surface is evident via Cl^- image, which is consistent with the AFM image [Fig. 6(b)] showing the surface of the vancomycin film deposited on the underneath PLGA layer. Therefore, TOF-SIMS is a powerful technique to identify molecules (and elements) and their three-dimensional locations with a lateral resolution of ∼2 μm and a depth resolution of 1 nm.

Finally, we show TOF-SIMS imaging of a sample made by placing a droplet of a solution of both PLGA and vancomycin in DMSO. Figures 8(a) and 8(b) shows images of $C_6H_7O_4{}^-$ and $C_7H_4O_2Cl^-$, representing PLGA and vancomycin, respectively. It is clear that vancomycin and PLGA were phase separated. We clarified that the observed phase separation between vancomycin and PLGA is associated with the solvent DMSO, as evidence by the image of $SO_3{}^-$ (80) in Fig. 8(c), which can be used to trace DMSO, the only chemical containing sulfur in the system. Because $SO_3{}^-$ was only detected in the vancomycin phase, indicating that the solvent was either incorporated into or reacted with vancomycin. On the other hand, the lack of $SO_3{}^-$ in the PLGA

phase indicates that the solvent evaporated from PLGA molecules. We also confirmed this finding for PLGA in DMSO and vancomycin in DMSO by spin-coating their respective solution on to a mica surface.

As discussed earlier, TOF-SIMS imaging of phase separated vancomycin and PLGA revealed that vancomycin may be impacted by DMSO. Because DMSO is an excellent solvent for many organic materials,[34,35] including vancomycin and
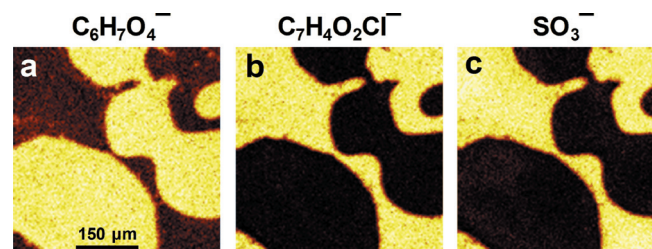

FIG. 8. Images of $C_6H_7O_4{}^-$ (a), $C_7H_4O_2Cl^-$ (b), and $SO_3{}^-$ (c), showing phase separation between PLGA and vancomycin, as well as association of DMSO with vancomycin. The sample was made from their solution in DMSO.

PLGA, it may be widely used in controlled-release drug delivery systems containing these two chemicals. More generally, for applications where vancomycin molecules need to adhere to alloys[36] or bacteria,[37] the use of DMSO may have a significant impact to their interactions. Therefore, investigations on possible impacts of DMSO to the antibiotic functionality of vancomycin may be warranted.

IV. CONCLUSIONS

We applied TOF-SIMS to investigate the ion fragmentation of vancomycin (molecular formula $C_{66}H_{75}Cl_2N_9O_{24}$, denoted as M), an antibiotic against Gram-positive bacteria. We identified two diagnostic ions $C_6H_{14}N^+$ and $C_7H_4O_2Cl^-$, whose abundance are approximately three quarters and one third of those of their most abundant ions $C_3H_8N^+$ and CN^-, respectively. Although much weaker than the two diagnostic ions, protonated molecular ion $[M+H]^+$ and decarboxylated molecular ion $[M-COOH]^-$ are also detected from vancomycin. We also demonstrated that TOF-SIMS is powerful in molecular imaging phase separated vancomycin and poly(lactide-*co*-glycolide) (PLGA) and depth profiling layered PLGA/vancomycin/PLGA structures. Our results are expected to promote applications of TOF-SIMS in investigating surface chemistry and chemical structures of controlled-release drug delivery systems involving vancomycin in a polymer matrix.

ACKNOWLEDGMENTS

[1]C. Schäffer and P. Messner, Microbiology **151**, 643 (2005).

[2]D. P. Levine, Clin. Infect. Dis. **42**, S5 (2006).

[3]Z. B. Yang, E. R. Vorpagel, and J. Laskin, J. Am. Chem. Soc. **130**, 13013 (2008).

[4]P.-A. Ashford and S. P. Bew, Chem. Soc. Rev. **41**, 957 (2012).

[5]Z. G. Jia, M. L. O'Mara, J. Zuegg, M. A. Cooper, and A. E. Mark, Biophys. J. **101**, 2684 (2011).

[6]N. K. Varde and D. W. Pack, Expert Opin. Biol. Ther. **4**, 35 (2004).

[7]P. Gao, X. Nie, M. J. Zou, Y. J. Shi, and G. Cheng, J. Antibiot. **64**, 625 (2011).

[8]H. K. Makadia and S. J. Siegel, Polymers **3**, 1377 (2011).

[9]L. Du, S. Y. Yang, W. Q. Li, H. Y. Li, S. B. Feng, R. Zeng, B. Yu, H.-Y. Nie, and M. Tu, Mater. Sci. Eng., C **78**, 1172 (2017).

[10]L. Wang *et al.*, J. Biomater. Appl. **31**, 995 (2017).

[11]C. M. Murphy, F. J. O'Brien, D. G. Little, and A. Schindeler, Eur. Cells Mater. **26**, 120 (2013).

[12]S. Bose, M. Roy, and A. Bandyopadhyay, Trends Biotechnol. **30**, 546 (2012).

[13]M. Lovett, K. B. Lee, A. Edwards, and D. L. Kaplan, Tissue Eng., Part B **15**, 353 (2009).

[14]Z. Pan and J. D. Ding, Interface Focus **2**, 366 (2012).

[15]A. Benninghoven, Angew. Chem. Int. Ed. Engl. **33**, 1023 (1994).

[16]J. S. Fletcher, N. P. Lockyer, S. Vaidyanathan, and J. C. Vickerman, Anal. Chem. **79**, 2199 (2007).

[17]J. C. Vickerman and N. Winograd, Int. J. Mass Spectrom. **377**, 568 (2015).

[18]C. M. Mahoney, Mass Spectrom. Rev. **29**, 247 (2010).

[19]H.-Y. Nie, Anal. Chem. **82**, 3371 (2010).

[20]V. Thiel and P. Sjövall, Annu. Rev. Earth Planet. Sci. **39**, 125 (2011).

[21]A. M. Belu, M. C. Davies, J. M. Newton, and N. Patel, Anal. Chem. **72**, 5625 (2000).

[22]G. L. Fisher, A. M. Belu, C. M. Mahoney, K. Wormuth, and N. Sanada, Anal. Chem. **81**, 9930 (2009).

[23]A. Pelster, B. J. Tyler, M. Körsgen, R. Kassenböhmer, R. E. Peterson, M. Stöver, W. E. S. Unger, and H. F. Arlinghaus, Biointerphases **11**, 041001 (2016).

[24]C. M. Mahoney, A. J. Fahey, A. M. Belu, and J. A. Gardella, Jr., J. Surf. Anal. **17**, 299 (2011).

[25]Q. P. Vanbellingen, A. Castellanos, M. Rodriguez-Silva, I. Paudel, J. W. Chambers, and F. A. Fernandez-Lima, J. Am. Soc. Mass Spectrom. **27**, 2033 (2016).

[26]A. Rafati *et al.*, J. Controlled Release **162**, 321 (2012).

[27]E. Belissa, C. Nino, M. Bernard, T. Henriet, H. Sadou-Yaye, E. Surget, G. Boccadifuoco, N. Yagoubi, and B. Do, J. Chromatogr. Sep. Tech. **5**, 1000243 (2014).

[28]J. Diana, D. Visky, J. Hoogmartens, A. Van Schepdael, and E. Adams, Rapid Commun. Mass Spectrom. **20**, 685 (2006).

[29]M. Zhang, G. A. Moore, and S. W. Young, J. Anal. Bioanal. Tech. **5**, 196 (2014).

[30]J. C. Vickerman, Analyst **136**, 2199 (2011).

[31]P. Bampoulis, K. Sotthewes, M. H. Siekman, H. J. W. Zandvliet, and B. Poelsema, Sci. Rep. **7**, 43451 (2017).

[32]J. C. L. Erve, M. Gu, Y. D. Wang, W. DeMaio, and R. E. Talaat, J. Am. Soc. Mass Spectrom. **20**, 2058 (2009).

[33]Q. Z. Hu, R. J. Noll, H. Y. Li, A. Makarov, M. Hardman, and R. G. Cooks, J. Mass Spectrom. **40**, 430 (2005).

[34]I. D. Brown, J. Solution Chem. **16**, 205 (1987).

[35]M. Montagna, Y. Jeanvoine, R. Spezia, and E. Bodo, J. Phys. Chem. A **120**, 4778 (2016).

[36]O. P. Edupuganti *et al.*, Bioorg. Med. Chem. Lett. **17**, 2692 (2007).

[37]C. Assmann, J. Kirchhoff, C. Beleites, J. Hey, S. Kostudis, W. Pfister, P. Schlattmann, J. Popp, and U. Neugebauer, Anal. Bioanal. Chem. **407**, 8343 (2015).